

# Noncollinear parametric generation in $\text{LiIO}_3$ and $\beta$ -barium borate by frequency-doubled femtosecond Ti:sapphire laser pulses

Vitaly Krylov and Alexander Kalintsev

*S. I. Vavilov State Optics Institute, Saint Petersburg 199034, Russia*

Alexander Rebane, Daniel Erni, and Urs P. Wild

*Physical Chemistry Laboratory, Swiss Federal Institute of Technology, ETH-Zentrum, CH-8092 Zürich, Switzerland*

Received August 19, 1994

In  $\text{LiIO}_3$  and BBO crystals the wave-matching conditions for femtosecond noncollinear parametric light generation at  $\lambda = 390$  nm pumping wavelength are investigated. In the  $\text{LiIO}_3$  crystal simultaneous phase- and group-velocity-matching angles are determined. Parametric generation occurred at  $0.45\text{--}2.9\text{-}\mu\text{m}$  wavelengths by pumping with the second harmonic of 150-fs Ti:sapphire laser pulses and is in qualitative agreement with calculated directions in both crystals.

Parametric nonlinear optical processes are useful in extending the tunability range of femtosecond lasers over the entire visible, near-UV, and near-IR regions. It has been demonstrated<sup>1-4</sup> that nonlinear crystals such as KTP, LBO, and BBO placed in an optical oscillator cavity and pumped synchronously with  $10^8\text{--}10^9$ -Hz repetition-rate femtosecond pulses of an energy of  $10^{-6}\text{--}10^{-9}$  J can produce broadly tunable femtosecond pulses. Femtosecond Ti:sapphire regenerative amplifiers currently provide pulse energies of the order of  $10^{-3}$  J near 800-nm wavelength at kilohertz repetition rates.<sup>5</sup> It is thus of great interest to convert this high-power femtosecond radiation into tunable visible light.

In Refs. 6-8 optical parametric amplification schemes using BBO crystals pumped by 0.15-1.0-mJ energy pulses at 620-nm wavelength were shown to produce short femtosecond pulses in the near IR under wavelength-noncritical phase-matching conditions. To achieve optimum parametric amplification of broadband femtosecond pulses, in addition to the phase matching, conditions for group-velocity matching also have to be fulfilled.

We report theoretical and experimental investigation of resonator-free noncollinear optical parametric generation in  $\text{LiIO}_3$  and BBO crystals (type I matching) pumped with  $\lambda = 390$ -nm frequency-doubled pulses of an amplified femtosecond Ti:sapphire laser. We demonstrate that for this interaction in  $\text{LiIO}_3$  not only phase-matching but also group-velocity-matching conditions are achieved. A schematic of our experimental setup is shown in Fig. 1. The 150-fs-duration spectrally transform-limited output pulses of the amplified Ti:sapphire laser (CPA-1, Clark-MXR, Inc.) with center wavelength  $\lambda = 780$  nm and with 0.8 mJ of energy per pulse are frequency doubled in a 2.5-mm-thick KDP crystal with a conversion efficiency of 30%. Color filter F1 eliminates the fundamental near-IR wavelength. The UV second-harmonic beam at  $\lambda = 390$  nm is directed to a  $\text{LiIO}_3$  crystal

(thickness  $h = 3$  mm, crystal cut angle  $\theta = 60^\circ$ ) or to a BBO crystal ( $h = 1.5$  mm,  $\theta = 31^\circ$ ) mounted upon a rotating stage. The energy of second-harmonic pump pulses is  $240\ \mu\text{J}$ , and the diameter of the unfocused beam is 5 mm. The second color filter, F2, stops the UV pump light while allowing the longer wavelengths to propagate to a white paper screen positioned at some distance behind the nonlinear crystal. The pattern of the generated parametric waves is observed in the form of colored rings centered around the propagation axis of the pump beam. We measure the angle of the cone,  $\alpha$ , the angular divergence  $\Delta\alpha$ , and the intensity of different generated wavelengths as a function of the phase-matching angle  $\theta$  between the pump beam's propagation direction in the crystal and the crystal symmetry axis.

Figure 2 shows the calculated and the experimentally measured noncollinear type I phase-matching and group-velocity-matching wavelengths for different angles in  $\text{LiIO}_3$  at the pump wavelength  $\lambda_p = 390$  nm. In the case of noncollinear parametric gen-

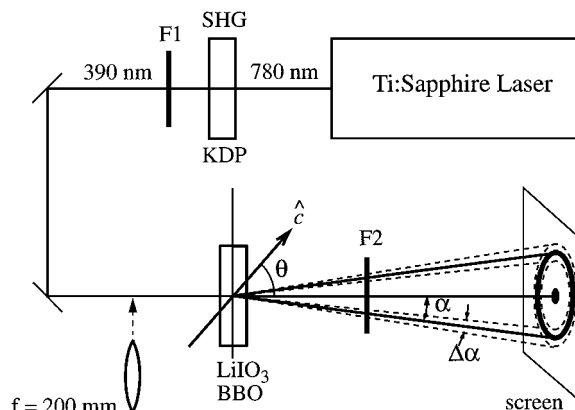


Fig. 1. Experimental setup: F1, F2, colored glass filters;  $\theta$ , angle between the direction of pump beam propagation and the crystal axis;  $\alpha$ , propagation angle of the parametric waves.

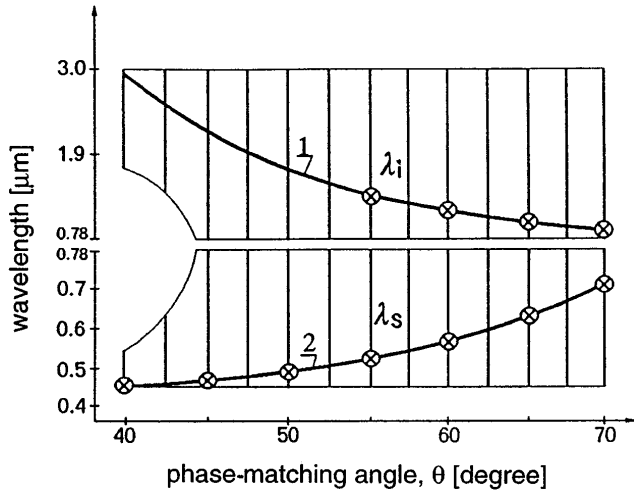


Fig. 2. Dependence of the wavelengths of noncollinear phase matching and group-velocity matching on the propagation direction of the pump beam in a  $\text{LiIO}_3$  crystal. The results of our calculations are shown as solid curves. Experimental data points are marked with  $\otimes$ 's.

eration the signal wave ( $\lambda_s$ ) and the idler wave ( $\lambda_i$ ) are propagating on conical surfaces having a common axis that coincides with the direction of propagation of the pump beam.<sup>9,10</sup> The areas in Fig. 2 marked by vertical solid lines indicate that for a given angle phase matching is satisfied for signal and idler waves simultaneously in a broad range of wavelengths. For the angles  $40^\circ < \theta < 44^\circ 30'$  the spectrum of the parametrically generated waves is partially limited, but for the angles  $\theta > 44^\circ 30'$  the whole spectrum between 450 nm and  $2.9 \mu\text{m}$  can be generated simultaneously.

Curves 1 and 2 of Fig. 2 show the wavelengths at which, in addition to phase matching, group-velocity matching of the interacting waves also occurs. The threshold for parametric generation of femtosecond pulses is expected to be lowest if both the phase- and the group-velocity-matching conditions are fulfilled. Indeed, the experimentally measured data for the  $\text{LiIO}_3$  crystal at the pump intensity  $I = 5 \text{ GW cm}^{-2}$  closely follow the calculated curve. We see that the spread of the simultaneously generated spectrum is much narrower than expected from the phase-matching condition alone. We also see that, because the group-velocity matching cannot be achieved at wavelengths close to the degenerate regime, no parametric generation is observed in the region of 700–880 nm at our pump intensities.

Figure 3 shows the calculated and the experimentally measured dependence of angle  $\alpha$  of the signal wave in  $\text{LiIO}_3$  at the group-velocity-matching wavelength as a function of the phase-matching angle  $\theta$ . When the crystal is tuned between the phase-matching angles  $40^\circ$  and  $70^\circ$ , then, because of the group-velocity matching, angle  $\alpha$  of the maximum emitted intensity increases from  $2.5^\circ$  to  $12^\circ$ . Simultaneously the maximum signal wavelength is tuned from 450 to 700 nm. It should be noted that the angles  $\theta$  and  $\alpha$  in Figs. 2 and 3 (and also Figs. 5 and 6 below) are given for beams propagating inside the crystal.

It follows from curves 1 and 2 of Fig. 2 that a larger angular divergence of the pump beam should lead to a broader spectrum of the parametrically generated signal in  $\text{LiIO}_3$ . It is also clear that increasing the spectral width of the pump beam also increases the spectral width of the parametric waves. Indeed, in our experiment with a spectral width of the pump beam  $\Delta\lambda_p = 5 \text{ nm}$  and a divergence of  $3'$  the signal wave had a spectral width of  $\Delta\lambda_s = 10 \text{ nm}$  in the region of 500 nm and of  $\Delta\lambda_s = 50 \text{ nm}$  in the region of 700 nm. The angular divergence  $\Delta\alpha$  changed from  $10'$  to  $1^\circ$  with a minimum divergence near  $\theta = 45^\circ$ . When the phase-matching angle was  $40^\circ < \theta < 45^\circ$ , the shorter-wavelength components of the signal wave propagated at larger  $\alpha$  than did the longer-wavelength components. At the angles  $\theta > 45^\circ$  this is reversed in accordance with the phase-matching condition. The polarization of the parametric waves was orthogonal to the polarization of the pump beam, which is expected for type I phase matching.

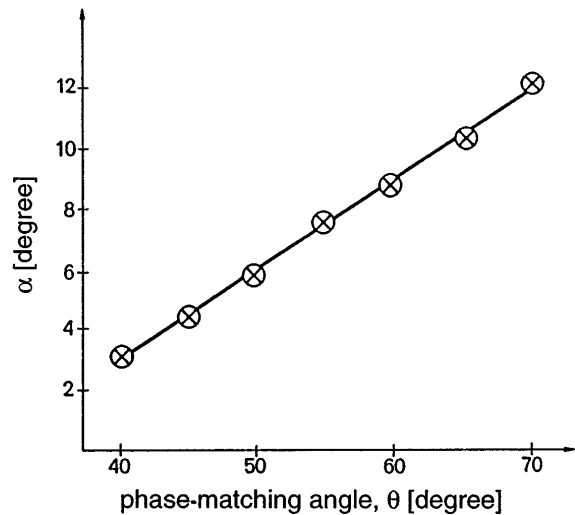


Fig. 3. Propagation angle  $\alpha$  of the parametric signal wave in  $\text{LiIO}_3$  as a function of the phase-matching angle.  $\otimes$  is experimental data.

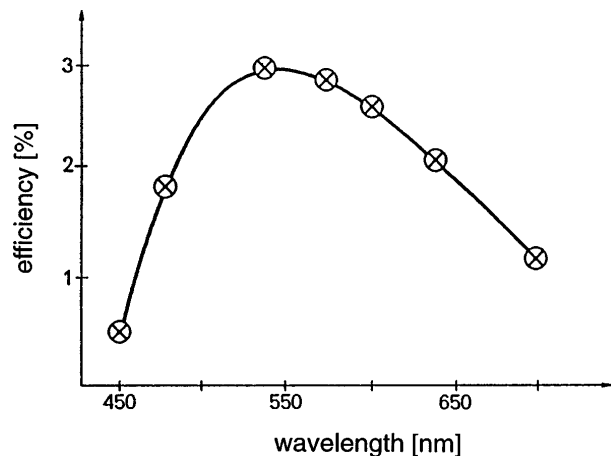


Fig. 4. Experimentally measured energy-conversion efficiency of the pump beam into the signal wave in  $\text{LiIO}_3$  at different maximum wavelengths. The energy of the parametric wave is integrated over all cone angles.

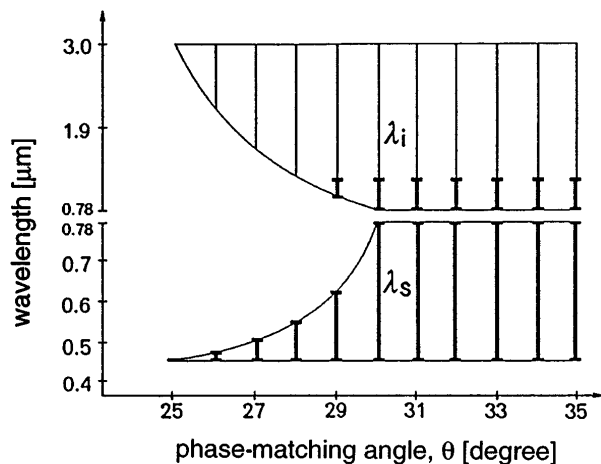


Fig. 5. Dependence of the wavelengths of noncollinear phase matching on the propagation direction of the pump beam in a BBO crystal. The results of our calculations are shown as thin solid lines. Experimentally observed wavelengths are marked with bold vertical solid lines.

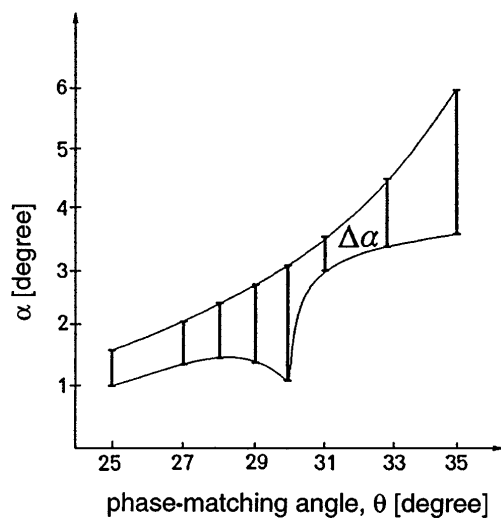


Fig. 6. Propagation angle and divergence of the parametric signal wave in BBO at different phase-matching angles. The calculated allowed generation angles are between the two thin solid curves. Bold vertical solid lines are the experimentally observed angles.

Figure 4 shows the experimentally observed conversion efficiency of the pump beam into a signal wave in the  $\text{LiIO}_3$  crystal with the emitted parametric wave energy integrated over all cone directions at different maximum wavelengths. We estimate that the intensity of the pump beam  $I = 5 \text{ GW/cm}^2$  is greater by a factor of 10 than the threshold intensity for the noncollinear parametric generation in this crystal.

Figures 5 and 6 show the calculated and the experimentally measured noncollinear parametric generation wavelengths and propagation angles as a function of the phase-matching angle in BBO crystal. Unlike for  $\text{LiIO}_3$ , in this nonlinear crystal group-velocity matching at the given pump wavelength is not possible. The pump intensity threshold for noncollinear parametric generation was  $I = 80 \text{ GW/cm}^2$ , and we achieved it by focusing the UV beam with a spherical lens of  $f = 200 \text{ mm}$ . Figure 5 shows that when the phase-matching angle was changed from

$25^\circ$  to  $30^\circ$  the spectral width of the signal wave increased from  $450 \text{ nm} < \lambda_s < 460 \text{ nm}$  to  $450 \text{ nm} < \lambda_s < 780 \text{ nm}$ . Figure 6 shows how angle  $\alpha$  and the divergence of the parametric radiation changed as the phase-matching angle was varied. At  $\theta = 31^\circ$  the divergence of the signal beam was minimal. When the synchronism angle was larger than  $30^\circ$  the whole spectrum from  $450 \text{ nm}$  to  $2.9 \mu\text{m}$  was simultaneously generated (our measuring apparatus allowed us to detect wavelengths below  $1.2 \mu\text{m}$ ). At  $\theta = 30^\circ$ , in a similar manner to that described above for the  $\text{LiIO}_3$  crystal, switching of the relative propagation angles of the short- and long-wavelength components in the parametric signal wave occurred.

In conclusion, we have presented experimental results on noncollinear parametric wave generation by pumping with high-energy femtosecond pulses at a wavelength of  $390 \text{ nm}$  that are in qualitative agreement with the calculated phase- and group-velocity-matching conditions in  $\text{LiIO}_3$  and BBO crystals. It should be noted that in our experiment the more conventional collinear optical parametric process was not observed. In the case of  $\text{LiIO}_3$  crystal this can be explained by the fact that, because simultaneous phase and group-velocity matching is fulfilled for the noncollinear process and not for the collinear parametric generation, the threshold for the latter process is higher and is not able to compete with noncollinear generation. For the BBO crystal, however, for which we also observed only noncollinear generation, a different explanation has to be found. Here we note only that at our pump intensity of  $80 \text{ GW/cm}^2$  in the crystal, self-focusing and filamentation of the laser beam are already taking place. These aspects of light generation are the subject of our further investigations.

This research was supported by the Swiss Priority Program of Optical Sciences, Applications and Technologies.

## References

1. D. C. Edelstein, E. S. Wachman, and C. L. Tang, *Appl. Phys. Lett.* **54**, 1728 (1989).
2. R. Laenen, H. Graener, and A. Laubereau, *Opt. Lett.* **15**, 971 (1990).
3. G. Mak, Q. Fu, and H. M. van Driel, *Appl. Phys. Lett.* **60**, 542 (1992).
4. H. M. van Driel, A. Hache, and G. Mak, *Proc. Soc. Photo-Opt. Instrum. Eng.* **2041**, 50 (1993).
5. F. Salin, J. Squire, G. Mourou, and G. Vaillancourt, *Opt. Lett.* **16**, 1964 (1991).
6. W. Joosen, H. J. Bakker, L. D. Noordam, H. G. Muller, and H. B. van Linden van den Heuvell, *J. Opt. Soc. Am. B* **8**, 2537 (1991).
7. W. Joosen, P. Agostini, G. Petite, J. P. Chambaret, and A. Antonetti, *Opt. Lett.* **17**, 133 (1992).
8. R. Danelius, A. Piskarskas, A. Stabinis, G. P. Banfi, P. Di Trapani, and R. Righini, *J. Opt. Soc. Am. B* **10**, 2222 (1993).
9. D. Magde, R. Scarlet, and H. Mahr, *Appl. Phys. Lett.* **11**, 381 (1967).
10. J. Falk and J. E. Murray, *Appl. Phys. Lett.* **14**, 245 (1969).